Structural and optical properties of β-Ga_2O_3 thin films grown by plasma-assisted molecular beam epitaxy

Susmita Ghose[a] and Md. Shafiqur Rahman
Material Science, Engineering and Commercialization Program, Texas State University, San Marcos, Texas 78666

Juan Salvador Rojas-Ramirez, Manuel Caro, and Ravi Droopad
Ingram School of Engineering, Texas State University, San Marcos, Texas 78666

Abraham Arias and Nicola Nedev
Institute of Engineering, Autonomous University of Baja California, Benito Juarez Blvd. esq. Calle de la Normal S/N, 21280 Mexicali, B.C., Mexico

(Received 13 November 2015; accepted 2 February 2016; published 19 February 2016)

Epitaxial beta-gallium oxide (β-Ga_2O_3) has been deposited on c-plane sapphire by plasma-assisted molecular-beam epitaxy technique using two methods. One method relied on a compound Ga_2O_3 source with oxygen plasma while the second used elemental Ga source with oxygen plasma. A side-by-side comparison of the growth parameters between these two methods has been demonstrated. With various substrate temperatures, pure phase $(\bar{2}01)$ oriented β-Ga_2O_3 thin films were obtained using both sources. Reflection high energy electron diffraction patterns displayed a three-fold reconstruction during the growth. X-ray photoelectron spectroscopy analysis showed a shift in the binding energy of the Ga 2p peaks consistent with a Ga being in a +3 oxidation state. For transparent oxide like β-Ga_2O_3, it is important to determine the index of refraction (n) and its functional dependence on the wavelength. The Cauchy dispersion relation was employed to evaluate the refractive index, film thickness, roughness values, and extinction coefficient. The band gap energies of the thin films were calculated to be ~5.02 eV by extrapolating the linear portion of Tauc-plot analysis and the refractive index is ~1.89 at the wavelength (λ) of 6328 Å, suggesting high structural quality and packing density of the oxide films. © *2016 American Vacuum Society*.
[http://dx.doi.org/10.1116/1.4942045]

I. INTRODUCTION

Due to their important electrical and optical properties, semiconductor oxides have attracted strong attention for various applications such as flat-panel displays, optical windows,[1] high temperature chemical gas sensors,[2] and dielectric layers.[3] While some transparent conductive oxides such as In_2O_3, SnO_2, ZnO, and ITO can be useful for some applications, their small bandgaps (~3 eV) are not suitable for devices operating in the UV wavelength region.[4] On the other hand, beta-gallium oxide (β-Ga_2O_3) represents the most promising oxide semiconductor material, due to its wide band gap (~4.9 eV) making it highly transparent from the visible to UV wavelength. Moreover, there has been significant progress in the use of β-Ga_2O_3 for high-power electronics with a high breakdown electric field of 8 MV/cm, which is larger than Si, GaN, or SiC, the most popular semiconductor materials for high-power device applications.[5] Additionally, β-Ga_2O_3 possesses a Baliga figure of merit (BFOM) higher than that of 4H-SiC and GaN with a projected maximum bulk electron mobility of 300 cm^2/V s.[5,6] The BFOM is associated with low specific on-resistance of a vertical electronic device and thus, making β-Ga_2O_3 ideal for low loss, high-voltage switching applications, including high-breakdown Schottky diodes and field-effect transistors.[5] Depending on the growth conditions, it is possible to vary its conductivity from insulator to conductor[1,7] making it more suitable for prospective applications in luminescent phosphors,[8] high temperature sensors,[2,9] antireflection coatings, and UV optoelectronics.[10] There are five different structures by which Ga_2O_3 can be crystallized and those are α, β, γ, δ, and ε phases. The most chemically and thermally (melting point at 1780 °C) stable structure that is suitable for device applications is the monoclinic β-Ga_2O_3 phase.[10] The lattice parameters of β-Ga_2O_3 are a = 12.23 Å, b = 3.04 Å, and c = 5.80 Å with a lattice angle $\beta = 103.7°$ and space group C2/m.[10–12] In prior reports, a variety of substrates including glass, quartz, Si, GaAs, BeO, and sapphire (Al_2O_3) were used to deposit β-Ga_2O_3. Among them, sapphire exhibits the smallest lattice mismatch while providing an insulating substrate.[13] To fabricate the β-Ga_2O_3 thin films, various techniques have been used including plasma-enhanced atomic layer deposition,[14,15] sputtering,[7,10] chemical-vapor deposition (CVD),[16,17] metalorganic CVD,[18] electron beam evaporation,[3] molecular-beam epitaxy (MBE),[4,6,19] and pulsed laser deposition.[20]

MBE can provide an ultrahigh vacuum environment and source materials which are of high purity so that the impurity levels of the grown films can be reduced significantly. Plasma assisted molecular beam epitaxy (PAMBE) represents an appropriate technology for the growth of high quality β-Ga_2O_3 single crystalline thin films, because it is well known for: (1) the reduction of the film impurity levels with an ultrahigh vacuum environment using high purity source

[a]Electronic mail: s_g333@txstate.edu

materials and (2) the control of atomic-layer growth through *in situ* monitoring by reflection high energy electron diffraction (RHEED). The lower unintended impurity levels in the epitaxial films allow for the investigation of the unexplained conduction mechanism with reproducible doping control through the improvement of the crystalline quality.[13,21]

In this paper, we reported on the epitaxial growth of single crystal β-Ga_2O_3 thin films on c-plane (0001) sapphire substrate by PAMBE method using two different sources with oxygen plasma: a compound Ga_2O_3 source material and the second using an elemental Ga. The properties of the Ga_2O_3 films, including chemical composition, optical properties, and surface morphology, were investigated and have been compared between these two sources. The use of a compound Ga_2O_3 source will introduce a new methodology of fabricating β-Ga_2O_3 thin films. There have been few prior investigations that have been reported using compound Ga_2O_3 source, so an understanding of the properties of the film will be useful for future investigation on the electrical properties of β-Ga_2O_3 through doping or band-engineering.

II. EXPERIMENT

Growths were carried out in an oxide MBE chamber with a base pressure of $<5 \times 10^{-10}$ Torr using a combination of turbomolecular and cryopumps. Effusion sources include a high temperature cell with an Ir crucible for the Ga_2O_3 polycrystalline source. In addition, oxygen was supplied from a radio frequency (RF) plasma source with a DC bias on the deflector plate to minimize the ions from reaching the substrate. During growth, the chamber cryopanels were cooled with LN_2 with the cryopump valved off when the plasma source was used. The growth was monitored *in situ* using RHEED.

In the present work, β-Ga_2O_3 films were deposited on single-side polished quarter of 2 in. c-plane sapphire substrates by PAMBE technique. The sapphire substrate was degreased in acetone for 10 min and thermally cleaned for 15 min at 800 °C in the growth chamber. In order to remove the adsorbates from the surface of the substrate, an additional oxygen plasma treatment was used for 40 min. To fabricate β-Ga_2O_3 thin films, one method included the use of Ga evaporated from an effusion cell with oxygen plasma generated through the RF activated radical cell. The second method used a compound polycrystalline Ga_2O_3 source, evaporating from an iridium crucible in a high temperature effusion cell with oxygen plasma. When Ga_2O_3 source is heated to a temperature of approximately 1800 °C (thermocouple temperature), it decomposes into gaseous components of Ga_2O and O_2. These by products were used to grow β-Ga_2O_3 with a much lower heat of formation when compared to the use of elemental Ga. In this study, substrate temperatures were varied from 650 to 750 °C for Ga elemental source and 700 to 850 °C when using the Ga_2O_3 compound source. For both growth methods, the oxygen gas flow rate and the input RF plasma power of the radical cell were maintained at 1.24 sccm and 300 W, respectively, resulting in a chamber pressure of 1×10^{-5} Torr during growth.

Various characterization techniques were employed to investigate the structural and optical properties, and chemical compositions of the films. The crystalline quality of the films were determined by means of a Bruker D8 Advance x-ray diffractometer (XRD) using Cu Kα ($\lambda = 1.5405$ Å) radiation. The surface morphology and roughness of the films were measured using atomic force microscope (AFM) operated in a contact mode. The chemical compositions and Ga oxidation states were determined using x-ray photoelectron spectroscopy (XPS) with a Mg x-ray source. To investigate the optical properties, spectroscopic ellipsometry (SE) measurements were performed employing a J.A. Wollam, M-2000 variable angle ellipsometer.

III. RESULTS AND DISCUSSION

Prior work on the use of Ga_2O_3 in a device structure involved the growth of an amorphous layer on GaAs for unpinning the Fermi level leading to the development of a compound semiconductor MOSFET technology.[22] In this technology, the Ga_2O_3 layer was deposited by MBE with polycrystalline Ga_2O_3 material from a high temperature cell and an iridium crucible. The use of this method was critical for the formation of the unique bonding at the interface that resulted in a low interface state density. The Ga_2O molecule emanating from the heated source was determined to be responsible for the Fermi level unpinning that could not be achieved through the use of elemental Ga and oxygen. Since the source contains oxidized Ga, it would suggest the growth of crystalline Ga_2O_3 thin films would require less energy and hence can be carried out at a lower temperature. A simple calculation of the heat of formation for Ga_2O_3 gives ΔH to be 20.76 kJ/mole when using Ga_2O and oxygen and 203.6 kJ/mole when using Ga and oxygen. This suggests that it would be more energetically favorable to grow Ga_2O_3 using the compound source.

To investigate the surface quality and growth mode of β-Ga_2O_3 thin film, the RHEED patterns were monitored during the growth. Upon Ga_2O_3 nucleation on sapphire substrate, the RHEED pattern initially showed a diffuse background. It was then followed by streaky RHEED patterns showing a threefold reconstruction with Kikuchi lines, irrespective of the growth methods used. Figure 1 shows a typical RHEED pattern showing a faint threefold reconstruction, indicating crystalline films' growth.

To investigate the crystal structure of the grown β-Ga_2O_3 thin films, θ-2θ x-ray diffraction patterns were recorded in the 2θ range of 15°–100°. Figure 2 shows XRD patterns of the films grown at various temperatures using the two sources (compound Ga_2O_3 source and elemental Ga source). The spectra contains four diffraction peaks corresponding to the $(\bar{2}01)$, $(\bar{4}02)$, $(\bar{6}03)$, and $(\bar{8}04)$ planes of β-Ga_2O_3 at 18.98°, 38.48°, 59.28°, and 82.30°. Apart from these peaks, no other peaks representing other Ga_2O_3 phases were found in scan range. This indicates that the thin films grown on c-plane sapphire are pure single phase $(\bar{2}01)$ oriented β-Ga_2O_3 similar to what was reported for β-Ga_2O_3 thin films grown on c-plane sapphire substrates, GaN substrates and a-plane

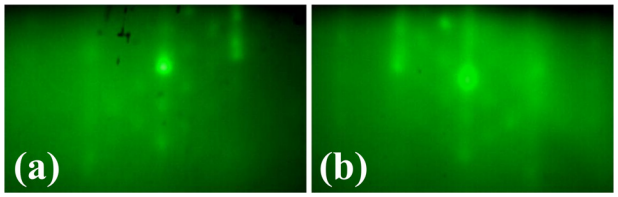

FIG. 1. (Color online) RHEED patterns during the growth of β-Ga_2O_3 using (a) compound Ga_2O_3 source and (b) elemental Ga source.

sapphire substrates.[23–25] For the films grown with elemental Ga, the spectra appeared to be similar when the growth temperature was increased from 650 to 750 °C [Fig. 2(b)]. However, the Ga_2O_3 peak intensity increased with growth thickness as expected from the spectra shown in Fig. 2(b) for the 3 h growth at 700 °C. In contrast, for the growth using compound Ga_2O_3 source, as shown in Fig. 2(a), there appeared to be a strong dependence on thickness with the growth temperature above 750 °C. With the growth temperature of 700 to 750 °C, the high intensity of the planes of β-Ga_2O_3 suggested that enough thermal energy is supplied to the molecules and atoms to increase the surface mobility, leading to a $(\bar{2}01)$ crystal orientation. According to previous studies, the arrangement of oxygen atoms of c-plane sapphire substrate is the same as in the $(\bar{2}01)$ plane of β-Ga_2O_3 resulting in the epitaxial relationship in which the $(\bar{2}01)$ β-Ga_2O_3||(0001) sapphire.[25,26] The gallium atoms bond to the oxygen atom layer of the sapphire substrate with smaller mismatch between the (0001) planes of the sapphire and the $(\bar{2}01)$ plane of β-Ga_2O_3.[24] By increasing the substrate temperature to 850 °C, the intensities of $(\bar{2}01)$ and higher order diffractions peaks from β-Ga_2O_3 decrease probably due to the decrease in film thickness, which result from a reduction in sticking coefficient of the Ga_2O molecules [Fig.2(a)]. The peaks located at 41.78° and 90.88° are the (006) and (0012) diffraction peaks of the c-plane sapphire substrate, respectively.

To investigate the stoichiometry and oxidation state of the grown β-Ga_2O_3 thin films, x-ray photoelectron spectroscopy was used. Figure 3 shows the survey scan for two films grown using the different sources with only the oxygen peak and Ga related peaks being present. To determine the oxidation state of Ga, the Ga 2p region was selected as shown in Fig. 4 for the compound source and the elemental Ga source.

The sum of Gaussian peaks on a Shirley background is used for the deconvolution of XPS spectrum, as shown in Fig. 4. The measured Ga 2p peak for the compound Ga_2O_3 source [Fig. 4(a)] grown at a temperature of 700 °C is a convolution of three peaks that can be assigned to Ga_2O_3 at binding energy (BE) of 1117.89 eV, Ga_2O at 1116.84 eV position, and elemental Ga at 1116.34 eV. The spectrum in Fig. 4(b) for Ga_2O_3 grown using elemental Ga at a temperature of 700 °C is a convolution of two peaks that can be assigned to Ga_2O_3 at 1117.32 eV and elemental Ga at 1116.03 eV. Shifting of binding energy occurs because of the redistribution of electrons around the constituent atoms of the crystal. So, the changes in chemical bonding results in shifting of binding energy which is used to infer information about the oxidation state of the Ga-oxide phases.[27] The oxidation states of +3, +1, and 0 for Ga that is present in the

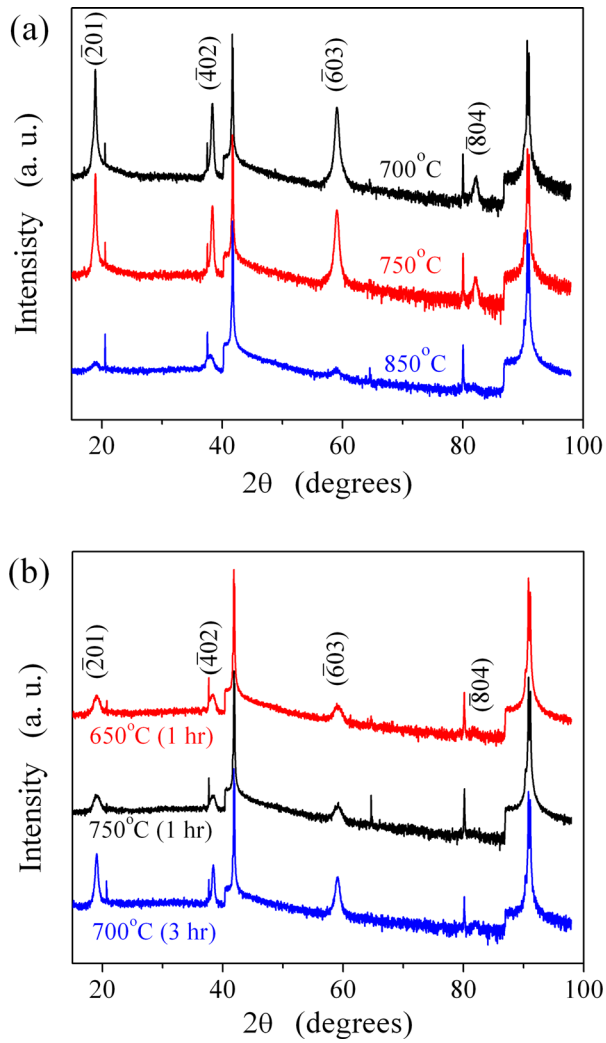

FIG. 2. (Color online) XRD patterns of β-Ga_2O_3 thin films grown using (a) compound Ga_2O_3 source and (b) elemental Ga source.

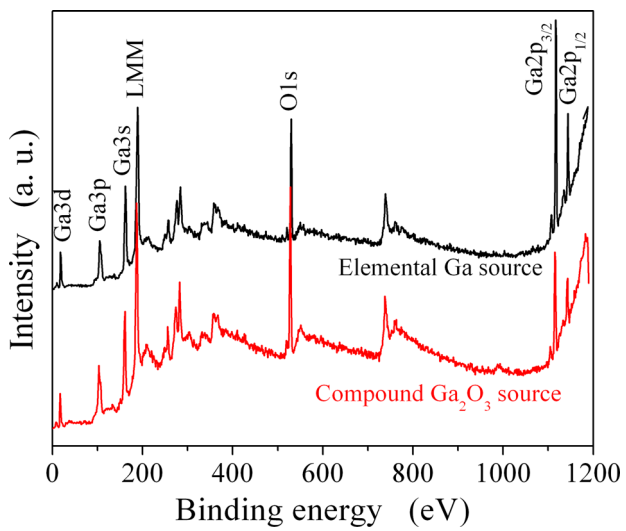

FIG. 3. (Color online) XPS survey scans of representative grown β-Ga_2O_3 films.

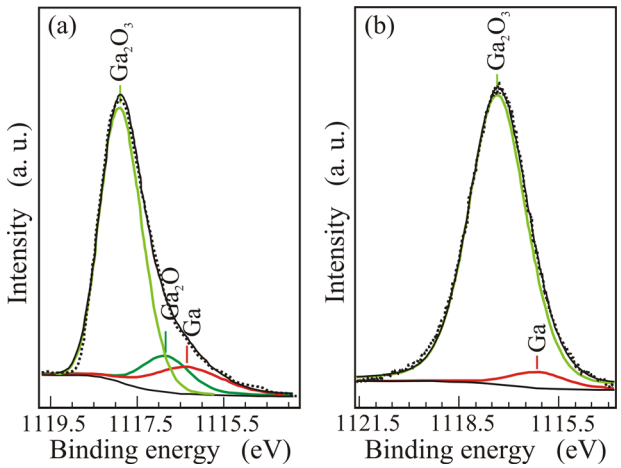

FIG. 4. (Color online) XPS of Ga 2p core level spectra of grown β-Ga_2O_3 thin films using (a) compound Ga_2O_3 source and (b) elemental Ga source. Experimental data are represented by dotted lines.

spectrum shown in Fig. 4(a) is probably due to the high growth temperature using the compound source. This high growth temperature reduces the sticking coefficient and oxidation of the Ga_2O molecule. It can also lead to some decomposition of the Ga_2O molecule of the surface, leading to the observation of a small amount of unoxidized Ga atoms. The reduction in the sticking coefficient can also be observed in the XRD spectra of Fig. 2(a) where the intensity of the Ga_2O_3 peaks is increased with reduced growth temperatures possibly due to an increase in the thickness of the oxide layers. On the other hand, the growth using elemental Ga requires higher temperatures for the complete oxidation of the Ga atoms based on the heat of formation.

Figure 5 shows a typical O 1s spectrum obtained from the grown films. This can be fitted with a single peak suggesting a film that is composed of Ga with a predominantly single oxidation state.

Scanning probe microscopy (Park XE7) in the AFM mode was used to investigate the effect of growth temperature on the surface morphology. AFM images were acquired at a scanning frequency of 1.5 Hz with a scanning area of $2 \times 2\ \mu m^2$. Figure 6 shows the AFM topographies of the surface of the films grown by both elemental Ga source and compound Ga_2O_3 source with different growth temperature. It is reported that the morphological characteristic of thin films highly depend on the growth conditions, including growth temperature and oxygen partial pressure.[23,24] The surface of the thin films deposited by PAMBE were found flat and smooth without obvious cracks or discontinuities for both sources. The root mean square (RMS) surface roughness of the films grown using compound Ga_2O_3 source with growth temperatures of 700, 750, and 850 °C are 2.71, 3.07, and 0.88 nm, respectively [Figs. 6(a)–6(c)], whereas the RMS surface roughness of the corresponding films grown using elemental Ga source with growth temperatures of 650, 700, and 750 °C are 0.37, 1.11, and 0.39 nm, respectively [Figs. 6(d)–6(f)], by PAMBE technique.

Optical properties such as the complex index of refraction, the dielectric constants, and thickness of the thin films were analyzed using SE by determining the ellipsometric parameters Ψ and Δ as a function of wavelengths (200–1000 nm) and incident angles (65°,70°, 75°, 80°, and 85°) at room temperature. A physical representation of the measured sample was constructed by a four layer model (analysis software CompleteEase, J. A. Woollam) through a step-by-step method. In order to analyze the optical properties of the thin film with respect to a substrate/film structure, the optical response of the c-plane Al_2O_3 substrate was first determined followed by the optical properties of β-Ga_2O_3 thin film. Subsequently, the measured ellipsometric data were fitted to the corresponding optical model generated data, depicted in Fig. 7(a). A minimum root mean square error was obtained by varying the parameters of the model during the fitting procedure expressed as[10]

$$\mathrm{RMSE} = \sqrt{\frac{1}{2n-m-1}\sum_{i=1}^{n}[(\Psi_i^{\mathrm{cal}}-\Psi_i^{\mathrm{exp}})^2+(\Delta_i^{\mathrm{cal}}-\Delta_i^{\mathrm{exp}})^2]}. \quad (1)$$

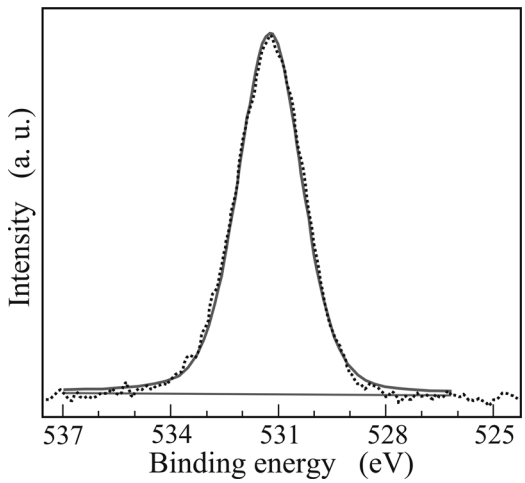

FIG. 5. O 1s core level spectra of Ga_2O_3 thin films. Experimental data (solid squares) was fitted to a single peak (solid line).

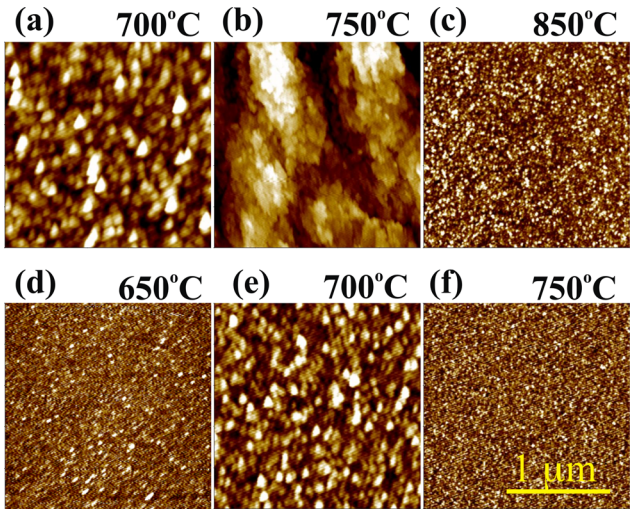

FIG. 6. (Color online) $2 \times 2\ \mu m^2$ AFM images of β-Ga_2O_3 films grown using [(a)–(c)] compound Ga_2O_3 source and [(d)–(f)] elemental Ga source.

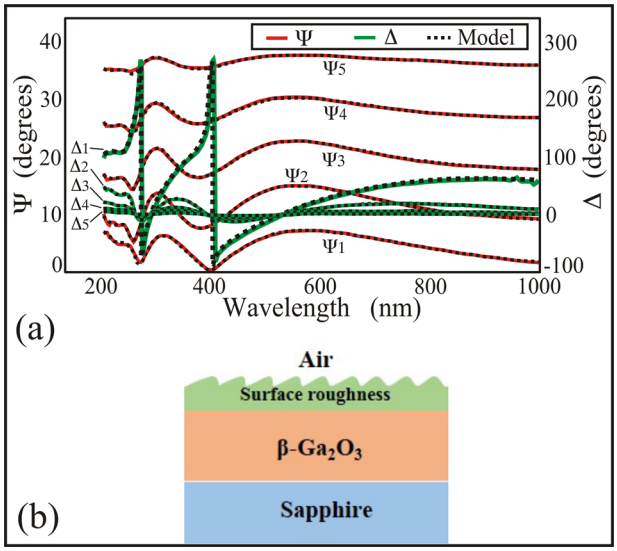

FIG. 7. (Color online) (a) Raw SE data (experimental-colored lines) and the corresponding calculated fittings (black dotted lines) as a function of wavelength. Curves Δ_1 and Ψ_1 were taken at an incident angle of 65°, Δ_2 and Ψ_2 at 70°, Δ_3 and Ψ_3 at 75°, Δ_4 and Ψ_4 at 80°, and Δ_5 and Ψ_5 at 85°. (b) Four layer model structure for β-Ga_2O_3.

Here, n is the number of data points in the spectra, m is the number of variable parameters in the model, and "exp" and "cal" denote the experimental and the calculated data, respectively.

Figure 7(b) sketches a four-medium optical model consisting of a semi-infinite c-plane Al_2O_3 substrate/β-Ga_2O_3 film/surface roughness/air ambient structure employed to investigate the β-Ga_2O_3 thin film where the roughness layer is employed to simulate the effect of surface roughness of the β-Ga_2O_3 film on the SE measurement. Since the optical constants for the c-plane Al_2O_3 substrate layer have been obtained separately, the free parameters correspond to the β-Ga_2O_3 film thickness, surface roughness layer thickness, and the β-Ga_2O_3 optical constants. The β-Ga_2O_3 optical constants are described by the Cauchy dispersion relation model with the surface roughness layer modeled by a Bruggeman effective medium approximation using a mix of 50% β-Ga_2O_3 and 50% voids.[28] The β-Ga_2O_3 film and surface roughness layer thicknesses are consistent with the profilometer and RMS roughness values from the AFM measurement, respectively.

In order to derive the quantitative structural properties relationship to better understand the effect of microstructure on the optical properties, a further analysis of the measured optical spectra is performed, shown in Fig. 8. The absorption of β-Ga_2O_3 follows a power law, since it has a direct band gap expressed as[28]

$$(\alpha h\upsilon) = B(h\upsilon - E_g)^{1/2}, \quad (2)$$

where $h\upsilon$ is the energy of the incident photon, α the absorption coefficient, B the absorption edge width parameter, and E_g the band gap.

It is evident that in the high absorption region, $(\alpha h\nu)^2$ vs $h\nu$ results in linear plots, suggesting direct allowed

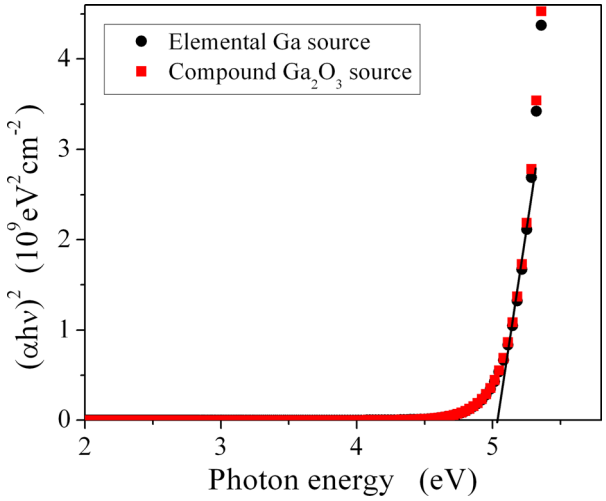

FIG. 8. (Color Online) Plots of $(\alpha h\nu)^2$ vs photon energy, $h\nu$ for the β-Ga_2O_3 epilayers deposited on sapphire. Optical direct bandgaps are estimated by extrapolation to $h\nu = 0$.

transitions across E_g of β-Ga_2O_3 films[4,10,28] with the band gap values determined by extrapolating the linear region of the plot to $h\nu = 0$. The bandgap found for elemental Ga source and compound Ga_2O_3 source is ~5.02 eV, which indicates an excellent optical transparency of the grown thin films in the UV and visible wavelength region. The refractive index, n (at wavelength of 6328 Å) calculated from SE data for β-Ga_2O_3 films, is ~1.89 eV. It is worth noting that the measured band gap energy values and the refractive indices in this work are comparable with those reported in the literature for β-Ga_2O_3.[10,15,28] A summary of the samples parameters is presented in Table I.

IV. CONCLUSIONS

High quality β-Ga_2O_3 thin films were grown on sapphire (0001) substrate by PAMBE technique using two different sources (elemental Ga source and compound Ga_2O_3 source) with oxygen plasma. A side-by-side comparison between these two source deposited films was demonstrated. XRD measurements indicated that the grown β-Ga_2O_3 film is single crystalline $(\bar{2}01)$ oriented for both sources. Streaky threefold RHEED reconstruction during growth is further evidence that the growth of the oxide films was single crystalline and

TABLE I. Comparison between two growth procedures (compound Ga_2O_3 source and elemental Ga source).

Growth temperature (°C)		Thickness (nm)	RMS roughness (nm)	Band gap (eV)	Refractive index at 632 nm
Ga_2O_3 compound source	700	161.50	2.71	5.02	1.91
	750	127.41	3.07	5.0	1.89
	850	15.89	0.88	5.01	1.79
Ga elemental source	650	23.22	0.37	4.96	1.76
	700	22.64	1.11	4.98	1.77
	750	23.22	0.39	5.02	1.77

epitaxial. XPS measurements showed a positive shift in the binding energy of the Ga 2p peaks consistent with a Ga being in a +3 oxidation state. Both XRD and XPS measurements indicated that the sticking coefficient reduces with increasing substrate temperature for compound Ga_2O_3 source. AFM images exhibited uniform and smooth surface for both sources. Spectroscopic ellipsometry has been used to evaluate and modeling the thickness and optical constants. The bandgap is found ~5.02 eV for both compound Ga_2O_3 source and elemental Ga source, which is indicative of high quality thin films.

[1]T. Minami, Semicond. Sci. Technol. **20**, S35 (2005).
[2]M. Fleischer and H. Meixner, Sens. Actuator, B **4**, 437 (1991).
[3]M. Passlack, N. E. J. Hunt, E. F. Schubert, G. J. Zydzik, M. Hong, J. P. Mannaerts, R. L. Opila, and R. J. Fischer, Appl. Phys. Lett. **64**, 2715 (1994).
[4]E. G. Víllora, K. Shimamura, K. Kitamura, and K. Aoki, Appl. Phys. Lett. **88**, 031105 (2006).
[5]M. Higashiwaki, K. Sasaki, A. Kuramata, T. Masui, and S. Yamakoshi, Appl. Phys. Lett. **100**, 013504 (2012).
[6]S. W. Kaun, F. Wu, and J. S. Speck, J. Vac. Sci. Technol., A **33**, 041508 (2015).
[7]P. Marie, X. Portier, and J. Cardin, Phys. Status Solidi A **205**, 1943 (2008).
[8]M. Fleischer and H. Meixner, Sensor Actuator, B **26**, 81 (1995).
[9]M. Ogita, K. Higo, Y. Nakanishi, and Y. Hatanaka, Appl. Surf. Sci. **175**, 721 (2001).
[10]C. V. Ramana, E. J. Rubio, C. D. Barraza, A. Miranda Gallardo, S. McPeak, S. Kotru, and J. T. Grant, J. Appl. Phys. **115**, 043508 (2014).
[11]K. Takakura, D. Koga, H. Ohyama, J. M. Rafi, Y. Kayamoto, M. Shibuya, H. Yamamoto, and J. Vanhellemont, Physica B **404**, 4854 (2009).
[12]C. Janowitz *et al.*, New J. Phys. **13**, 085014 (2011).
[13]D. Guo *et al.*, Opt. Mater. Express **4**, 1067 (2014).
[14]R. K. Ramachandran, J. Dendooven, J. Botterman, S. P. Sree, D. Poelman, J. A. Martens, H. Poelman, and C. Detavernier, J. Mater. Chem. A **2**, 19232 (2014).
[15]F. K. Shan, G. X. Liu, W. J. Lee, G. H. Lee, I. S. Kim, and B. C. Shin, J. Appl. Phys. **98**, 023504 (2005).
[16]G. A. Battiston, R. Gerbasia, M. Porchiaa, R. Bertoncellob, and F. Caccavale, Thin Solid Films **279**, 115 (1996).
[17]D. H. Kim, S. H. Yoo, K. S. An, H. S. Yoo, and Y. Kim, Bull. Korean Chem. Soc. **23**, 225 (2002).
[18]Y. Lv, J. Ma, W. Mi, C. Luan, Z. Zhu, and H. Xiao, Vacuum **86**, 1850 (2012).
[19]T. Oshima, O. Takeya, and F. Shizuo, Jpn. J. Appl. Phys. **46**, 7217 (2007).
[20]F. B. Zhang, K. Saito, T. Tanaka, M. Nishio, and Q. X. Guo, Appl. Phys. Lett. **387**, 96 (2014).
[21]M. Y. Tsai, O. Bierwagen, M. E. White, and J. S. Speck, J. Vac. Sci. Technol., A **28**, 354 (2010).
[22]R. Droopad, R. Karthik, A. Jon, A. Liz, N. England, D. Uebelhoer, P. Fejes, P. Zurcher, and M. Passlack, J. Cryst. Growth **301**, 139 (2007).
[23]S. L. Ou, D. S. Wuu, Y. C. Fu, S. P. Liu, R. H. Horng, L. Liu, and Z. C. Feng, Mater. Chem. Phys. **133**, 700 (2012).
[24]S. Müller, W. H. Von, D. Splith, F. Schmidt, and M. Grundmann, Phys. Status Solidi A **211**, 34 (2014).
[25]S. Nakagomi and K. Yoshihiro, J. Cryst. Growth **349**, 12 (2012).
[26]G. V. Chaplygin and S. A. Semiletov, Thin Solid Films **32**, 321 (1976).
[27]W. Priyantha, G. Radhakrishnan, R. Droopad, and M. Passlack, J. Cryst. Growth **323**, 103 (2011).
[28]M. Rebien, W. Henrion, M. Hong, J. P. Mannaerts, and M. Fleischer, Appl. Phys. Lett. **81**, 250 (2002).